

## Half-metallic ferromagnetism and spin polarization in CrO<sub>2</sub>

L. Chioncel,<sup>1,2</sup> H. Allmaier,<sup>2</sup> E. Arrighoni,<sup>2</sup> A. Yamasaki,<sup>3</sup> M. Daghofer,<sup>3</sup> M. I. Katsnelson,<sup>4</sup> and A. I. Lichtenstein<sup>5</sup>

<sup>1</sup>Department of Physics, University of Oradea, 410087 Oradea, Romania

<sup>2</sup>Institute of Theoretical Physics, Graz University of Technology, A-8010 Graz, Austria

<sup>3</sup>Max-Planck-Institut für Festkörperforschung, Heisenbergstrasse 1, D-70569 Stuttgart, Germany

<sup>4</sup>University of Nijmegen, NL-6525 ED Nijmegen, The Netherlands

<sup>5</sup>Institute of Theoretical Physics, University of Hamburg, DE-20355 Hamburg, Germany

(Received 29 March 2007; published 26 April 2007)

We present electronic structure calculations in combination with local and nonlocal many-body correlation effects for the half-metallic ferromagnet CrO<sub>2</sub>. Both zero temperature results from a variational cluster approach as well as finite-temperature dynamical mean field theory results support the existence of low-energy nonquasiparticle states, which turn out to be essential for a correct quantitative description of depolarization effects.

DOI: 10.1103/PhysRevB.75.140406

PACS number(s): 75.50.Cc, 71.20.Be, 71.10.-w

In recent years, magnetoelectronic devices have emerged that are able to exploit both the charge and the spin of electrons by means of spin-polarized currents and spin-dependent conduction.<sup>1,2</sup> The capabilities of these devices depend crucially upon the spin polarization of the underlying material. In this area, half-metallic ferromagnets are of particular interest, chromium dioxide CrO<sub>2</sub> is especially a strong candidate for magnetoresistance devices with a favorable switching behavior at small fields.<sup>3</sup>

Based on first-principles calculations, CrO<sub>2</sub> is classified as a half-metallic ferromagnet.<sup>4</sup> Point contact measurements at superconductor metal interfaces reveal a spin polarization of the conduction electrons larger than 90%,<sup>5,6</sup> supporting the half-metallic nature predicted by band theory.<sup>7</sup> In addition, CrO<sub>2</sub> fulfills yet another essential requirement for practical purposes, namely a high Curie temperature, determined experimentally in the range of 385–400 K.<sup>8</sup> The saturation magnetization at 10 K was reported to be 1.92  $\mu_B$  per Cr site,<sup>9</sup> which is close to the ideal value (2  $\mu_B$ ) and is consistent with half-metallicity. The magnetic susceptibility in the paramagnetic phase shows a Curie-Weiss-like behavior indicating the presence of local moments,<sup>10</sup> suggesting a mechanism of ferromagnetism beyond the standard band or Stoner-like model.

The band structure of CrO<sub>2</sub> has been calculated self-consistently within the local-spin-density-approximation (LSDA) by several authors. K.-H. Schwarz<sup>7</sup> predicted the half-metallic behavior for this material with a spin moment of 2  $\mu_B$  per formula unit. Later, several experiments including photoemission,<sup>11</sup> soft x-ray absorption,<sup>12</sup> resistivity,<sup>13</sup> and optics<sup>14</sup> have suggested that electron correlations are essential to understand the underlying physical picture in CrO<sub>2</sub>. In this spirit, LSDA+U calculations<sup>15</sup> have been used to study the effect of large on-site Coulomb interactions. These studies suggested that CrO<sub>2</sub> is a material with a negative charge-transfer gap which leads to self-doping. In contrast to the on-site strong correlation description, transport and optical properties obtained within the density functional theory using LSDA and generalized-gradient approximation<sup>16</sup> suggest that the electron-magnon scattering is responsible for the renormalization of the one-electron bands. More recent model calculations also suggest the importance of orbital correlations.<sup>17,18</sup>

An appropriate treatment of correlation effects, which goes beyond the mean-field LSDA+U treatment, is achieved in the framework of dynamical mean field theory (DMFT),<sup>19</sup> in which a *local* energy-dependent self-energy is adopted. However, nonlocal self-energy effects turn out to be important for a correct description of the so-called nonquasiparticle (NQP) states,<sup>20,21</sup> which are crucial for the depolarization in half-metallic ferromagnets.<sup>22–25</sup> For this reason, we present here a realistic electronic-structure calculation for CrO<sub>2</sub>, where nonlocal self-energy effects are treated within the variational cluster approach (VCA).<sup>26–29</sup> While the VCA calculation is currently limited to zero temperature, we also present finite-temperature results obtained within a DMFT description.

In order to achieve a realistic description of the material, the parameters of the correlated model Hamiltonian are determined via *ab initio* electronic-structure calculations. CrO<sub>2</sub> has a rutile structure with Cr ions forming a tetragonal body-center lattice. Cr<sup>4+</sup> has a closed shell Ar core and two additional 3d electrons. The Cr ions are in the center of the CrO<sub>6</sub> octahedra. Therefore, the 3d orbitals are split into a  $t_{2g}$  triplet and an excited  $e_g$  doublet. With only two 3d electrons, important correlation effects take place essentially in the  $t_{2g}$  orbitals, while  $e_g$  states can be safely neglected. The cubic symmetry is further reduced to tetragonal due to a distortion of the octahedra, which partially lifts the degeneracy of the  $t_{2g}$  orbitals into a  $d_{xy}$  ground state and  $d_{xz+zy}$  and  $d_{xz-zy}$  excited states.<sup>15,30</sup> We therefore restrict the VCA calculation to three orbitals on each site representing the Cr- $t_{2g}$  manifold described by the Hamiltonian

$$H = H_0 + \frac{1}{2} \sum_{i\{m,\sigma\}} U_{mm'm''m'''} c_{im\sigma}^\dagger c_{im'\sigma'}^\dagger c_{im''\sigma''} c_{im'''\sigma'''} \quad (1)$$

where  $c_{im\sigma}$  destroys an electron with spin  $\sigma$  on orbital  $m$  on site  $i$ . Here,  $H_0$  is the noninteracting part of the Hamiltonian restricted to the  $t_{2g}$  orbitals obtained by the downfolding procedure implemented within the  $N$ -order muffin-tin orbital (NMTO) method<sup>31,32</sup> using the local-density approximation (LDA). In this way, the effects of the remaining orbitals are included effectively by renormalization of hopping and on-site energy parameters. The on-site Coulomb-interaction

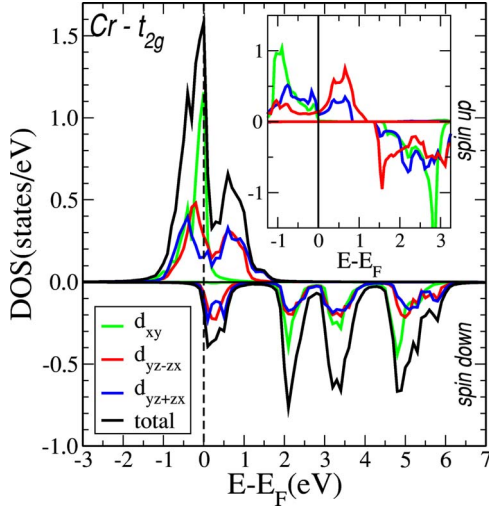


FIG. 1. (Color online) Cr- $t_{2g}$  orbital-resolved density of states in the ferromagnetic state, calculated within the LDA+VCA approach for  $U=3$  eV, and  $J=0.9$  eV. NQP states are visible in the minority spin channel, just above the Fermi energy. The inset shows the LDA+U density of states for the same parameters.

terms in Eq. (1) are expressed in terms of the diagonal direct coupling  $U_{mmmm}=U$ , the off-diagonal direct coupling  $U_{mm'mm'}=U'$ , and the exchange coupling  $U_{mm'm'm}=J$ .<sup>33</sup> Notice that spin-rotation invariance is automatically guaranteed by the form Eq. (1), i.e., spin-flip terms are also included in our calculation. The pair-hopping term is also included via  $U_{mm'm'm'}=J$ . The Coulomb-interaction ( $U$ ) and Hund's exchange ( $J$ ) parameters between  $t_{2g}$  electrons are evaluated from first principles by means of a constrained LSDA method.<sup>34</sup> While this method is not very accurate, and may produce slightly different values depending on its exact implementation, it is quite clear that for  $\text{CrO}_2$  the interaction parameters are not too strong. An appropriate choice is  $U \approx 3$  eV and  $J \approx 0.9$  eV. Corrections for a “double counting” of the interaction only produces an irrelevant constant shift of the chemical potential,<sup>35</sup> as we are considering a model Hamiltonian with fixed number of electrons.

The VCA accesses the physics of a lattice model in the thermodynamic limit by optimizing trial self-energies generated by a reference system. The reference system consists of an isolated cluster having the same interaction as the original lattice, but differing in the single-particle part of the Hamiltonian. An approximation to the self-energy of the lattice model is then obtained by finding the saddle point of an appropriate grand-canonical potential

$$\Omega = \Omega' + \text{Tr} \ln G_{\text{VCA}} - \text{Tr} \ln G_{cl} \quad (2)$$

with respect to the single-particle parameters of the reference system.<sup>27</sup> Here,  $G_{cl}$  is the Green's function matrix of the reference system (cluster), which is calculated numerically as a function of frequency and spin, using a zero-temperature Lanczos procedure. The lattice Green's function  $G_{\text{VCA}}$  is obtained by a matrix form of the Dyson equation, whereby the self-energy  $\Sigma$  of the reference system is used as an approximation to the lattice self-energy. Finally,  $\Omega'$  is the grand-canonical potential of the reference system.

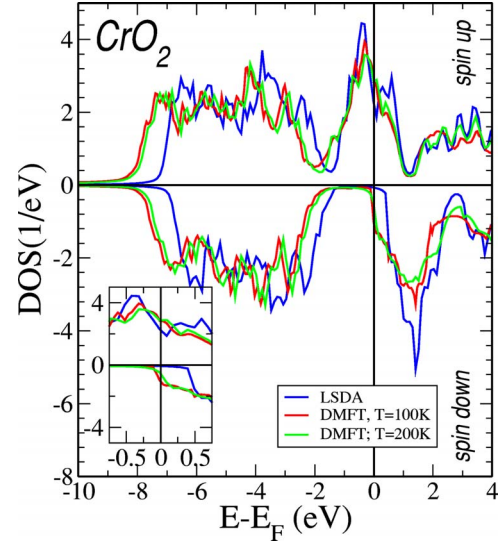


FIG. 2. (Color online) Density of states obtained within the LSDA and LSDA+DMFT calculations for different temperatures. The inset shows the results for a smaller energy window around the Fermi level.

As a reference system for the VCA calculation, we take a cluster of four sites located in the (110) plane, and containing two from each inequivalent  $\text{Cr}_1$  and  $\text{Cr}_2$  sites.<sup>36</sup> We have checked that our results do not change substantially when using a cluster of six sites. We stress that the remaining hoppings, namely the ones between  $\text{Cr}_1$ - $\text{Cr}_1$  along  $x$  and  $y$  are not neglected, but taken into account in the noninteracting lattice Green's function entering the Dyson equation in the expression for the VCA Green's function. Quite generally, multi-orbital strongly correlated systems show a competition between different magnetic and orbital-ordered phases. In order to check that the ferromagnetic phase is the one with the lowest energy, we have compared its grand-canonical potential with the one of different magnetic phases containing mixed antiferromagnetic and ferromagnetic components in different directions.<sup>36</sup> Notice that the particle density in the physical system is in general different from the one of the reference system;<sup>29</sup> the former turns out to be slightly doped with  $n=1.81$  particles per unit cell. Moreover, for the parameters we have used here, which are the appropriate ones for  $\text{CrO}_2$ , we confirm that the ferromagnetic state is more favorable energetically with respect to all antiferromagnetic states we have considered, as well as to the paramagnetic state.

In order to analyze the role of the different  $d$  orbitals, we present in Fig. 1 the orbital and spin-resolved density of states (DOS). For comparison, we show in the inset the results obtained within the mean-field-like LDA+U decoupling of the Hubbard interaction for the Cr- $t_{2g}$  orbitals.<sup>15</sup> In the LDA+U, a pseudogap feature opens at the Fermi energy in the majority (spin up) DOS, which is attributed to the crystal-field splitting between the  $d_{yz+zx}$  and  $d_{yz-zx}$  orbitals. This pseudogap is already present in the (uncorrelated) LSDA results shown in Fig. 2, although the effects of the interaction in LSDA+U enhance this effect. On the contrary, in the VCA calculation, correlation effects again reduce the pseudogap feature with respect to LSDA+U and shift it to higher energies.

A remarkable result of the VCA calculation is the presence of a significant amount of density of states at the Fermi energy originating from the putatively localized  $d_{xy}$  orbital. More specifically, we obtain that this orbital is not completely half filled, its occupation being  $n^{xy} \approx 0.87$ , while for the other two orbitals we have  $n^{yz+zx} \approx 0.49$ , and  $n^{yz-zx} \approx 0.45$ . This is confirmed by our LSDA+DMFT calculation, discussed below, for which  $n^{xy} \approx 0.87$ , and  $n^{yz+zx} \approx 0.46$ . Consequently, the  $d_{xy}$  orbital consists of quite itinerant electrons, although with a large effective mass, rather than of localized moments. Notice that our findings are in contrast to previous DMFT calculations,<sup>17,18</sup> in which the Fermi energy only touches the high-energy tail of the  $d_{xy}$  DOS, which can then be considered as localized moments. This is probably due to the large value of the interaction parameter  $U$  used in these calculations. We believe that the smaller value of  $U \approx 3$  eV used here is more appropriate, as it is obtained from first principles.

In the minority spin channel, NQP states are clearly visible predominantly in the  $d_{yz\pm zx}$  orbitals just above the Fermi energy. The physical origin of the NQP states is connected with the “spin-polaron” processes:<sup>20,21</sup> the spin-down low-energy electron excitations, which are forbidden for half-metallic ferromagnets in the one-particle picture, turn out to be possible as superpositions of spin-up electron excitations and virtual magnons.<sup>20,21</sup> A uniform superposition forms a state with the same total spin quantum number  $S=(N+1)/2$  ( $N$  is the particle number in the ground state) as the low-energy spin-up state, but with one “spin flip,” i.e., with  $z$ -component  $S_z=S-1$ . If the Hamiltonian is spin-rotation invariant, this state with one additional spin-down particle must have the same energy as the low-energy state with one additional spin-up particle, although its weight is reduced by a factor  $1/N$ . We stress that spin-rotation invariance is crucial in order to obtain low-energy NQP states. For this reason, methods neglecting spin flip processes in Eq. (1) are not expected to provide a correct description of NQP states. Similar NQP states are obtained in the fully self-consistent LSDA+DMFT calculation described in the following paragraph.

The above VCA calculation was carried out by starting from a model (1), whose parameters are obtained *ab initio* from electronic-structure calculations. This procedure does not take into account feedback effects of the correlation-induced charge redistribution into the LSDA potential. This is still a difficult task in a VCA calculation. In addition, correlations and states in the  $e_g$   $d$  orbitals are neglected. In order to explore the consequences of these effects, and to access finite temperatures, which is more difficult within a Lanczos-VCA approach, we also carried out a multi-orbital LSDA+DMFT calculation, which includes the full Cr  $d$  manifold, as well as a complete  $spd$ -basis set for all the atoms in the unit cell. In addition, we include both self-energy and charge self-consistency, which means that many-body effects are taken into account in the evaluation of the LSDA potentials. Details of this method have been given elsewhere.<sup>37</sup> All previous LSDA+ $U$  (Refs. 15 and 38) or DMFT (Refs. 17 and 18) studies, independently yield a narrow almost flat band of  $d_{xy}$  character which produces the ferromagnetic phase of  $\text{CrO}_2$ . We show that in contrast to

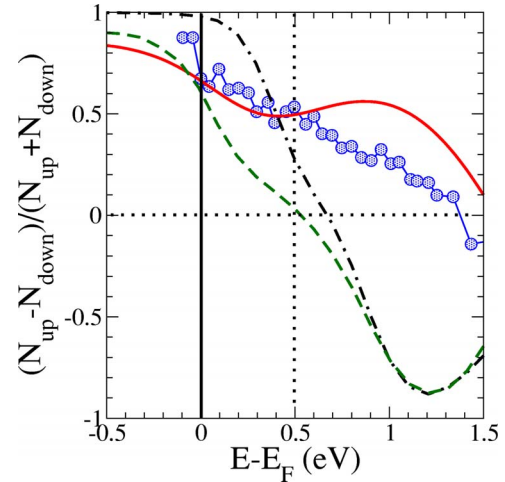


FIG. 3. (Color online) Energy dependence of the spin polarization obtained experimentally (Ref. 39, decorated solid line) and by different theoretical calculations LDA (dotted-dashed), DMFT (dashed), VCA (solid) [Eq. (3)]. A broadening of 0.4 eV, corresponding to the experimental resolution, has been added to the theoretical curves.

these previous results, the fully self-consistent LSDA+DMFT results, in agreement with the above nonlocal VCA approach, yields an itinerant  $d_{xy}$  orbital, which crosses the Fermi surface. It is interesting to note that despite the non-localized nature of the orbital, we still obtain a ferromagnetic phase.

The DOS obtained from our LSDA+DMFT calculation is presented in Fig. 2 for two different values of  $T$ , and compared with the LSDA results. As discussed above, the LSDA Fermi level intersects the majority-spin bands near a local minimum and lies in the band gap of the minority spin states. Finite temperatures and correlation effects close this minimum around the Fermi level, as can be seen from the LDA+DMFT results in Fig. 2. No differences can be observed between the two DMFT results at different temperatures, except for the smearing of DOS features at higher temperature. For both spin channels, the DOS is shifted uniformly to lower energies in the energy range of  $-2$  and  $-6$  eV, where predominantly the  $O(p)$  bands are situated. This is due to the fact that correlated Cr( $d$ ) bands affect the  $O(p)$  states through the Cr( $d$ )- $O(p)$  hybridization, so that the latter contribute actively to the mechanism of the ferromagnetic ground state. The LSDA+DMFT calculation confirms the existence of minority spin states just above the Fermi energy, as observed in the VCA calculation.

We now show that many-body effects discussed above, especially the formation of NQP states, contribute significantly to the energy dependence of the spin polarization

$$P(E) = [N_{\uparrow}(E) - N_{\downarrow}(E)] / [N_{\uparrow}(E) + N_{\downarrow}(E)], \quad (3)$$

where  $N(E)$  is the density of states of majority  $\uparrow$  or minority  $\downarrow$  electrons. Figure 3 shows a comparison between the measured<sup>39</sup> and computed polarization for the different *ab initio* many-body calculations discussed in the present paper. Due to the tails of NQP states, polarization is less than 100% even at the Fermi level. The LDA calculation clearly overes-



timates the spin polarization as it neglects correlation effects. On the other hand, both VCA and DMFT results show excellent agreement with the experiment at the Fermi level. At an energy of about 0.5 eV, polarization is reduced by about 50%, and up to this energy the agreement of the VCA calculation is excellent, while DMFT results overestimate depolarization effects away from the Fermi energy. The disagreement for energies above  $\approx 0.5$  eV is probably due to terms not included in the VCA Hamiltonian (1), such as  $e_g$  orbitals which start becoming important at higher energies.

In conclusion, we addressed the effects of electronic correlations in  $\text{CrO}_2$  and showed how these considerably change the picture obtained within LSDA and LSDA+U, despite the fact that the interaction is not very strong. More specifically, while in LSDA+U exchange and crystal-field splitting pin the  $\text{Cr}d_{xy}$  electrons become localized moments, the competition with charge fluctuation effects, which are taken into account in our DMFT and VCA calculations, induce a ferro-

magnetic state in which also  $d_{xy}$  electrons are itinerant, although with a large effective mass. We believe that this is the correct behavior at this intermediate value of the interaction parameters, which we derive *ab initio*, in contrast to results obtained with a larger value of  $U$ .<sup>15,17,18,38</sup> We show that correlation-induced NQP states, as well as an appropriate description of their nonlocal contributions to the self energy as obtained by VCA, are crucial for a correct description of the energy dependence of the polarization. Additional effects, such as, e.g., disorder or phonons, are also expected to contribute to the spin depolarization.

We thank C. Scheiber for help in the spin-rotation invariant part of the code. This work is supported by the Austrian Science Fund (FWF project P18505-N16). L.C. acknowledges financial support obtained through the Romanian National University Research Council CNCSIS Grant No. 96/2006.

- <sup>1</sup>G. A. Prinz, *Phys. Today* **48**(4), 58 (1995).
- <sup>2</sup>J. M. Daughton, A. V. Pohm, R. T. Fayfield, and C. H. Smith, *J. Phys. D* **32**, R169 (1999).
- <sup>3</sup>F. Y. Yang, C. L. Chien, E. F. Ferrari, X. W. Li, G. Xiao, and A. Gupta, *Appl. Phys. Lett.* **77**, 286 (2000).
- <sup>4</sup>R. A. de Groot, F. M. Mueller, P. G. van Engen, and K. H. J. Buschow, *Phys. Rev. Lett.* **50**, 2024 (1983).
- <sup>5</sup>R. Soulen, J. M. Byers, M. S. Osofsky, B. Nadgorny, T. Ambrose, S. F. Cheng, P. R. Broussard, C. T. Tanaka, J. Nowak, J. S. Moodera, A. Barry, and J. M. D. Coey, *Science* **282**, 85 (1998).
- <sup>6</sup>Y. Ji, G. J. Strijkers, F. Y. Yang, C. L. Chien, J. M. Byers, A. Anguelouch, G. Xiao, and A. Gupta, *Phys. Rev. Lett.* **86**, 5585 (2001).
- <sup>7</sup>K. Schwarz, *J. Phys. F: Met. Phys.* **16**, L211 (1986).
- <sup>8</sup>S. M. Watts, S. Wirth, S. von Molnár, A. Barry, and J. M. D. Coey, *Phys. Rev. B* **61**, 9621 (2000).
- <sup>9</sup>R. Yamamoto, Y. Moritomo, and A. Nakamura, *Phys. Rev. B* **61**, R5062 (2000).
- <sup>10</sup>B. Chamberland, *CRC Crit. Rev. Solid State Mater. Sci.* **7**, 1 (1977).
- <sup>11</sup>T. Tsujioka, T. Mizokawa, J. Okamoto, A. Fujimori, M. Nohara, H. Takagi, K. Yamaura, and M. Takano, *Phys. Rev. B* **56**, R15509 (1997).
- <sup>12</sup>C. B. Stagescu, X. Su, D. E. Eastman, K. N. Altmann, F. J. Himpsel, and A. Gupta, *Phys. Rev. B* **61**, R9233 (2000).
- <sup>13</sup>K. Suzuki and P. M. Tedrow, *Phys. Rev. B* **58**, 11597 (1998).
- <sup>14</sup>E. J. Singley, C. P. Weber, D. N. Basov, A. Barry, and J. M. D. Coey, *Phys. Rev. B* **60**, 4126 (1999).
- <sup>15</sup>M. A. Korotin, V. I. Anisimov, D. I. Khomskii, and G. A. Sawatzky, *Phys. Rev. Lett.* **80**, 4305 (1998).
- <sup>16</sup>I. I. Mazin, D. J. Singh, and C. Ambrosch-Draxl, *Phys. Rev. B* **59**, 411 (1999).
- <sup>17</sup>M. S. Laad, L. Craco, and E. Müller-Hartmann, *Phys. Rev. B* **64**, 214421 (2001).
- <sup>18</sup>L. Craco, M. S. Laad, and E. Müller-Hartmann, *Phys. Rev. Lett.* **90**, 237203 (2003).
- <sup>19</sup>A. Georges, G. Kotliar, W. Krauth, and M. J. Rozenberg, *Rev. Mod. Phys.* **68**, 13 (1996).
- <sup>20</sup>D. M. Edwards and J. A. Hertz, *J. Phys. F: Met. Phys.* **3**, 2191 (1973).
- <sup>21</sup>V. Y. Irkhin and M. I. Katsnelson, *J. Phys.: Condens. Matter* **2**, 7151 (1990).
- <sup>22</sup>L. Chioncel, M. I. Katsnelson, R. A. de Groot, and A. I. Lichtenstein, *Phys. Rev. B* **68**, 144425 (2003).
- <sup>23</sup>L. Chioncel, M. I. Katsnelson, G. A. de Wijs, R. A. de Groot, and A. I. Lichtenstein, *Phys. Rev. B* **71**, 085111 (2005).
- <sup>24</sup>L. Chioncel, E. Arrigoni, M. I. Katsnelson, and A. I. Lichtenstein, *Phys. Rev. Lett.* **96**, 137203 (2006).
- <sup>25</sup>L. Chioncel, Ph. Mavropoulos, M. Ležaić, S. Blügel, E. Arrigoni, M. I. Katsnelson, and A. I. Lichtenstein, *Phys. Rev. Lett.* **96**, 197203 (2006).
- <sup>26</sup>M. Potthoff, M. Aichhorn, and C. Dahnken, *Phys. Rev. Lett.* **91**, 206402 (2003).
- <sup>27</sup>M. Potthoff, *Eur. Phys. J. B* **36**, 335 (2003).
- <sup>28</sup>M. Aichhorn and E. Arrigoni, *Europhys. Lett.* **72**, 117 (2005).
- <sup>29</sup>M. Aichhorn, E. Arrigoni, M. Potthoff, and W. Hanke, *Phys. Rev. B* **74**, 024508 (2006).
- <sup>30</sup>S. P. Lewis, P. B. Allen, and T. Sasaki, *Phys. Rev. B* **55**, 10253 (1997).
- <sup>31</sup>O. K. Andersen and T. Saha-Dasgupta, *Phys. Rev. B* **62**, R16219 (2000).
- <sup>32</sup>A. Yamasaki, L. Chioncel, A. I. Lichtenstein, and O. K. Andersen, *Phys. Rev. B* **74**, 024419 (2006).
- <sup>33</sup>A. I. Lichtenstein and M. I. Katsnelson, *Phys. Rev. B* **57**, 6884 (1998).
- <sup>34</sup>V. I. Anisimov and O. Gunnarsson, *Phys. Rev. B* **43**, 7570 (1991).
- <sup>35</sup>E. Pavarini, S. Biermann, A. Poteryaev, A. I. Lichtenstein, A. Georges, and O. K. Andersen, *Phys. Rev. Lett.* **92**, 176403 (2004).
- <sup>36</sup>Details will be given elsewhere.
- <sup>37</sup>L. Chioncel, L. Vitos, I. A. Abrikosov, J. Kollar, M. I. Katsnelson, and A. I. Lichtenstein, *Phys. Rev. B* **67**, 235106 (2003).
- <sup>38</sup>A. Toropova, G. Kotliar, S. Y. Savrasov, and V. S. Oudovenko, *Phys. Rev. B* **71**, 172403 (2005).
- <sup>39</sup>D. J. Huang, L. H. Tjeng, J. Chen, C. F. Chang, W. P. Wu, S. C. Chung, A. Tanaka, G. Y. Guo, H.-J. Lin, S. G. Shyu, C. C. Wu, and C. T. Chen, *Phys. Rev. B* **67**, 214419 (2003).